Correlation between foam structure and mechanical performance of aluminium foam sandwich panels

Tillmann Robert Neu[1,2], Paul Hans Kamm[1,2], Nadine von der Eltz[1,2], Hans-Wolfgang Seeliger[3], John Banhart[1,2], Francisco García-Moreno[1,2]

[1] Institute of Materials Science and Technology, Technische Universität Berlin, Hardenbergstr. 36, 10623 Berlin, Germany

[2] Institute of Applied Materials, Helmholtz-Zentrum Berlin für Materialien und Energie, Hahn-Meitner-Platz 1, 14109 Berlin, Germany

[3] pohltec metalfoam GmbH, Robert-Bosch-Str. 6, 50769 Köln

Keywords

Aluminium Foam Sandwich, cellular material, X-ray imaging, mechanical properties, X-ray inspection

Abstract

Aluminium foam sandwich panels containing aluminium alloy sheets ('AFS') have been made available now in sizes up to a few square metres but an unresolved problem in production is how to cope with non-uniformities of the foam and the general lack of mechanical property data of AFS. We investigate large industrial AFS panels and test X-ray radiography as a method to identify weak points in the foam core. For samples in which defects are identified, correlation with failure in tensile and bending tests is investigated. The properties of a large number of samples tested in compression, tension and bending are determined and presented in AFS property tables. We find that X-ray radiography has the potential to identify flawed and potentially weak AFS panels and can be used to test 100 % of an industrial production output. The mechanical data measured for in total 120 samples provides a more reliable data base compared to the hitherto published sparse information.

Introduction

Metal foams are cellular materials consisting of a solid phase and a gaseous phase dispersed therein. As a result of their structure, they exhibit a combination of properties such as low density, favourable stiffness-to-mass ratio and good energy absorption properties. A sandwich design based on dense face sheets can yield compression, tension, torsion or bending properties beyond those of a metal foam alone. Face sheets protect the foam core from surface damage and corrosion, and allow the structure to bear tensile loads, where the bare metal foam performs poorly. An optimisation like this can also be carried out for other materials and yields structures such as honeycomb panels, stringer-

stiffened structures or waffle plates. However, such even stiffer structures are prone to earlier failure under certain shear stresses due to the engineered anisotropic nature of these materials. Metals foams have a more isotropic behaviour due to their more arbitrary structure [1][2][3].

Most of these structural materials are made for lightweight construction. The base material is often from the group of lightweight metals and most commonly an aluminium alloy. This combination makes it interesting for applications in transportation. The focus of this paper lies on aluminium foam sandwich (AFS®) panels. For the different production routes and the corresponding properties of metal foams see [4]. They have been proposed for use as crash absorbers for cars or trams, battery cases for electric cars, supports of working platforms on a mobile crane vehicle, train front structures or floors of a wagons [5][6]. Additionally, due to their excellent heat diffusion and conduction properties [7] it is also possible to use AFS as a thermal conductor for cooling systems [8].

Since a product rarely consists of only one part joints are an essential component and are usually subjected to larger loads and different stress modes. Joining of metal foams has been described in detail elsewhere [9]. Joining of a sandwich structure is facilitated by the face sheets, which can be joined by traditional sheet joining methods [1]. Due to the deformability of the AFS, the edge areas can be compressed to protect the foam inside from corrosion or mechanical penetration by external bodies and to allow for connections by, for example, screwing.

Reliable processing of AFS panels into products should be aided by this work. We show correlations of the structure observed by X-ray inspection and the mechanical properties measured by tension, compression and 4-point bending tests. It is demonstrated that X-ray inspection of the panels is a viable option as quality control in production. We also provide mechanical data of AFS measured on in total 120 samples.

Methods

All the samples were prepared from AFS panels produced by Pohltec Metalfoam GmbH (Cologne, Germany) through a patented process [10]. Precursor production consists of mixing metal and blowing agent powders, filling a container with the mixture, and compacting and rolling the container. The precursor can then be cut to size and foamed e.g. in an infrared furnace. The process is described in more detail elsewhere [11]. After foaming, however, the sandwich material is not completely flat due to locally occurring inhomogeneities in foam expansion. In order to guarantee a required flatness and thickness of an AFS, foamed panels (maximum dimensions of 2500 × 1100 mm) are levelled in a hot press at a temperature close to the solidus temperature of the alloy the foam core is made of. This ensures a flatness of 1 mm/m or better. The final foamed sandwich panels consist of two layers of dense aluminium alloy plates (EN AW 6082) metallically bonded to a foam

core of the alloy AlSi8Mg4 (in wt.%). The nominal thickness of the face sheets was 0.75 mm, that of the foamed core 6.5 mm. The non-levelled compression samples were produced using a thicker precursor layer leading to a foam core thickness of on average about 10 mm.

For applications where joining of parts is required, the panels were pressed down to a denser plate at selected locations. In this way, local strength was increased. To measure the properties in such areas, 400 mm × 400 mm large AFS plates were pressed down in a hot press, during which the overall thickness of the AFS plate was reduced to less than 4.8 mm.

Samples for mechanical testing were prepared using a CNC milling machine (High-Z S-720, CNC-STEP GmbH, Geldern, Germany), for tensile tests (parallel to the face sheets) and for 4-point bending tests according to the standards given in DIN 50125 – Shape E (tensile) and DIN 53293 (bending). To minimize compression of the foam due to the clamping forces the ends of the tensile test samples were reinforced with epoxy. The 10 pores in each direction in the samples for compression tests required according to DIN 50134 could be ensured only in the lateral directions due to the 2D nature of AFS panels. Samples had an area of either 40 mm × 40 mm (non-levelled AFS) or 25 mm × 25 mm (levelled AFS). See also Fig 2 a or b for basic directions and orientation. The thickness variations of non-levelled samples were no more than 0.15 mm, those of levelled samples 0.05 mm. After cutting, the samples were deburred, measured in size and mass, and X-ray radiographic images were taken. The foam core density of the samples was calculated using

$$\rho = \frac{M - M_{FS}}{V - V_{FS}},$$

where M and V are the total mass and volume of a specimen, while M_{FS} and V_{FS} are the mass and volume of the face sheets calculated by using nominal values.

The X-ray setup used for radiographic inspection consists of a micro-focus X-ray source from Hamamatsu Photonics (Hamamatsu, Japan) with a spot size of 5 µm and a power of 10 W (100 kV and 100 µA). The radiographic images were detected by a flat panel detector, also from Hamamatsu, with a 110 mm × 116 mm large field of view and 2240 × 2344 pixels, each one 50 µm × 50 µm in size. The sample was placed directly in front of the detector so that the geometrical magnification by the conical beam was negligible. The system is explained in detail elsewhere [12].

False colour images were calculated from the greyscale X-rays radiographs in two ways using self-written ImageJ scripts. The images were corrected with darkfield and flatfield images (Fig 1a), and the logarithm of each pixel grey value taken. The images were then divided into 50 × 50 pixel large segments in which the standard deviation of the grey values was calculated, coloured accordingly and superimposed over the original images with an opacity of 50 % (Fig 1b). For the density images, after taking the logarithm, the image was slightly blurred with a Gaussian filter to smoothen the

transitions, scaled to ±100 % and coloured using a lookup table (Fig 1c). In addition, contour lines were inserted for the range between -40 % and +40 % (Fig 1d).

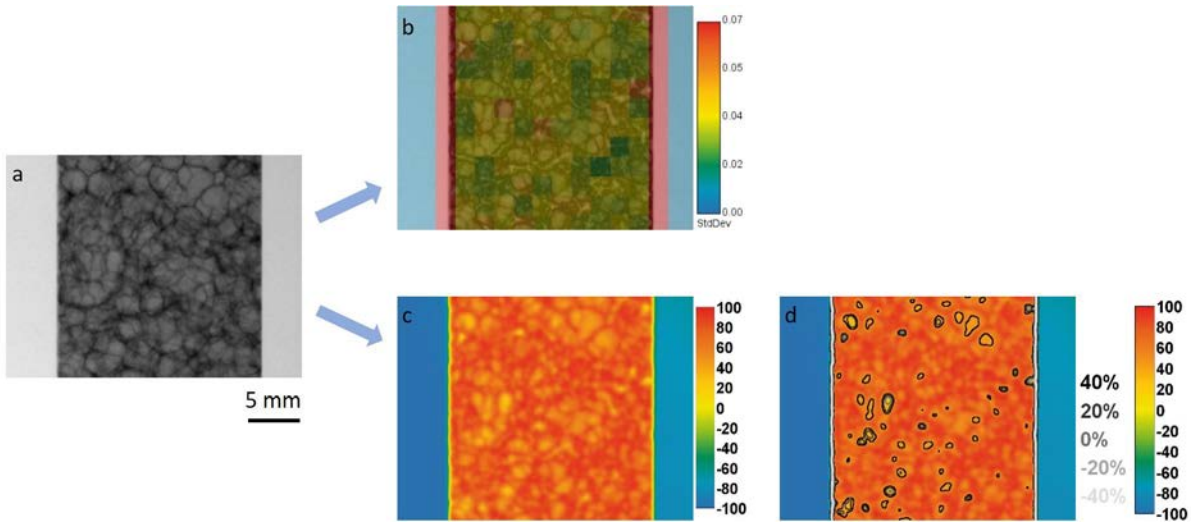

Fig 1 – a) corrected X-ray radiography b) colour overlay on the radiography based on the standard deviation of the logarithmic grey values in a 50 pixel × 50 pixel grid c) colouration of the radiography by logarithms of grey value and d) image from c with additional contour lines.

For some of the AFS samples, full tomography was performed by recording 1000 radiographic projections distributed over an angle of 360° with the same system just by placing a sample on a rotation stage from Huber (Rimsting, Germany). The projection images were reconstructed to a tomogram using Software Octopus (Inside Matters, Aalst, Belgium). Here, a geometrical magnification of 2.5× was used and round samples (cf. Fig 3) were milled out of the AFS to reduce artefacts in the reconstruction.

Mechanical tests were conducted using a RetroLine tC Vario with a maximum load of 20 kN and the software testControl II from ZwickRoell (Ulm, Germany) who also provided the tension, compression and 4-point bending kits. The quasi-static testing conditions were taken from the specific standards DIN EN ISO 6892-1 (tensile test), DIN 53291 (compression test) and DIN 53293 (4-point bending test) according to which the instrument software calculated mechanical values. All values given in figures tables and text are engineering values. The definition of the plateau stress from DIN 50134 was used and applied between 5 and 13 % strain. Between 20 and 25 samples for each condition were usually tested and analysed.

Results

Levelling

Levelling of foamed AFS panels is needed for most applications, because the AFS plate after foaming is not flat enough due to non-uniform expansion of the foam core. For this, the already solidified foam is mechanically levelled at temperatures close to its solidus temperature, where plastic flow is more likely than at 'room temperature'. Curved or kinked cell walls are repeatedly found in levelled specimens (compare Fig 2a and b). In panels which have been pressed down more severely, areas may have formed where cells are flattened and cell walls are folded into themselves (see Fig 2c on the left). Levelling will increase the core density. The amount varies depending on the core thickness and on the thickness reduction needed and lays usually between 5 and 15 %.

Densification

For mechanically stressed joints, the compression of the levelling process is continued until a denser compacted plate is produced with foam core densities reaching on average 1.55 ± 0.21 g/cm³. Cell walls are only rarely discernible here and occasionally a void can be found. This difference is also visible in the X-ray image (Fig 2d), where the transition from levelled to compacted AFS plate can be observed. While the foam structure is sharp on the levelled side, it becomes slightly blurred on the densified side.

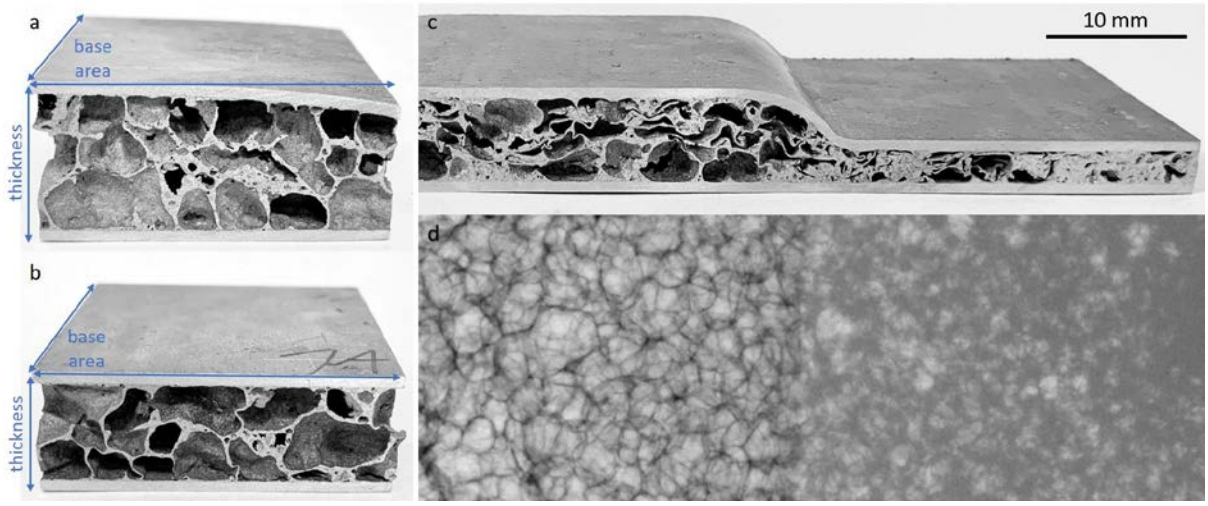

Fig 2 – Photographs of a) AFS piece as foamed, b) AFS piece after levelling, c) shaped AFS piece, partially densified at the sides and d) radiographic image (top view) of transition between levelled (left) and densified (right) areas.

The bands with flattened cells, which have also been described in the literature [13][14], have different preferred positions depending on the thickness of the AFS panel. While in thinner AFS panels they tend to be found close to the top and bottom face sheets, in thicker AFS panels they are

predominantly located in the centre, e.g. Fig 3a. This can be observed in the semi-transparent tomogram in Fig 3b where the pores were identified with the algorithm further described elsewhere [15]. The three major axes of each individual pore were determined using Principal Component Analysis [16], whereby a value for flatness ranging from 0 (flat) to 1 (round) was calculated from the ratio of the variances along the smallest and intermediate major axis (eigenvalues λ of the covariance matrix of the voxel set associated with a pore). Here, all pores with flatness below 0.4 are highlighted in red. One such band could be visually identified from the outside in over 90 % of the levelled samples.

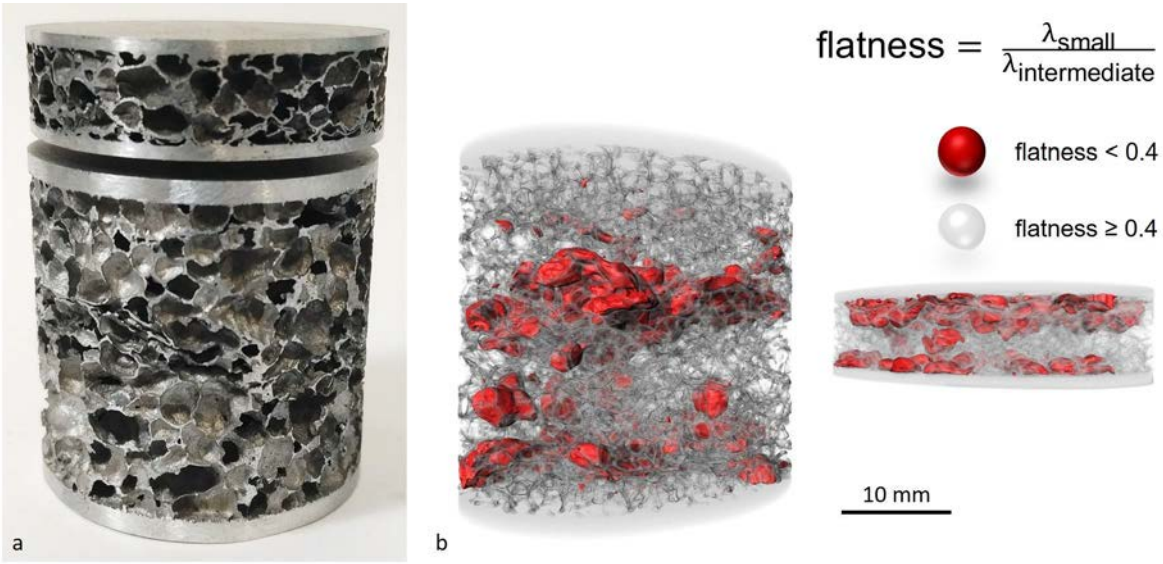

Fig 3 – Images of two levelled AFS samples of different thicknesses (10 mm and 30 mm) a) Photograph and b) 3D rendered images obtained by tomography: transparent visualisation with all pores highlighted in red that have a flatness lower than 0.4, while the remaining pores are kept in grey. Left/right in b) corresponds to bottom/top in a), respectively.

X-ray inspection

Since it is too time-consuming and expensive to perform a 3D quality control by tomography on a large number of AFS panels, we propose X-ray radiography as a way to inspect them in a non-destructive, fast and automated way and to find a correlation between their structure and mechanical properties. As shown in Fig 4, a full X-ray radiographic characterisation of a 1 m² large AFS panel known to contain some defects was simulated by cutting the panel into 25 tiles, of which the centres were examined by 25 X-ray radiographies, thus probing 32 % of the total area. This procedure was chosen because neither a large enough area detector nor a 1-m long line detector was available. The latter could be used in industrial applications to scan large panels.

The foam structure and local density are represented by the grey values of the detector. In the greyscale image (Fig 4a) some defects are already detectable visually. For example, some pores are

larger than the surrounding ones and some areas of uniform grey values in the bottom row of the image appear unusually structureless. These areas are even more clearly visible as blue regions in the overlay of the standard deviation (see Fig 4b, marked by red dashed circles). The standard deviation is zero if there is no structure in the examined sample that absorbs the X-rays to different extents. Inspection of the cut edges of the individual tiles shows that these areas are partially unfoamed regions, which are only in some cases visible from the side of the face sheets, e.g. through dents on the top layer, but mostly go unnoticed. How far such and other defects influence the mechanical values needs to be determined.

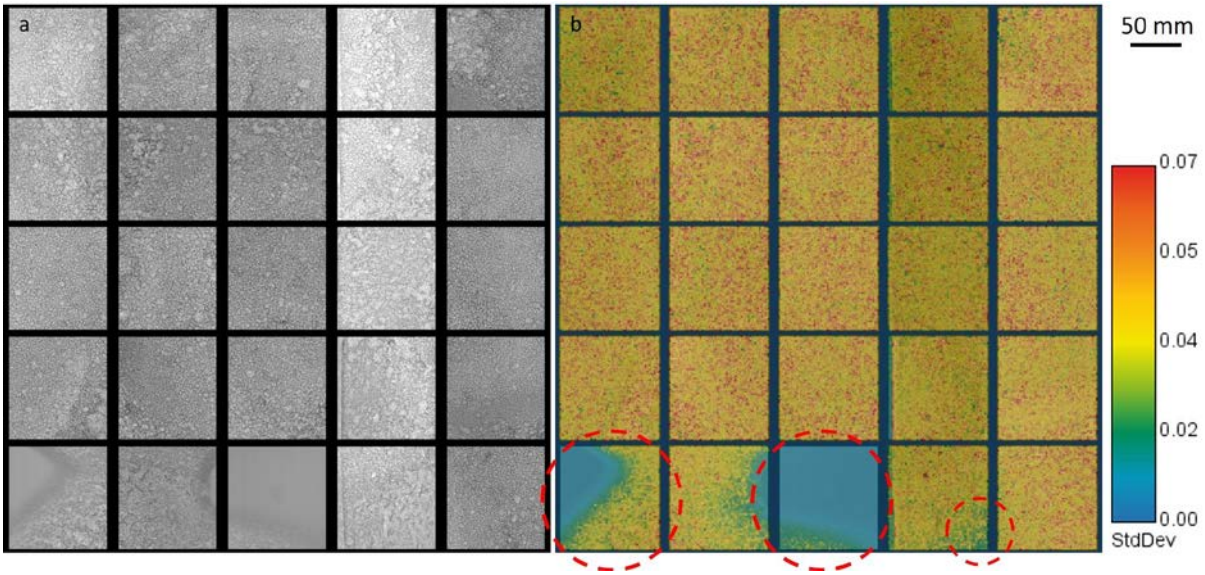

Fig 4 – Detailed non-destructive X-ray inspection of an AFS panel of 1000 mm × 1000 mm size. The entire inspected area is 550 mm × 580 mm large. The spaces between the individual tiles are shown in black and are not to scale. a) Greyscale X-ray radiographies and b) images colour coded by standard deviation revealing more clearly the structure of the core foam and poorly foamed regions marked by broken red circles.

Tensile tests

Tensile tests of both the levelled and the densified AFS panels parallel to the face sheets reveal ductile deformation behaviour (see Fig 5). The levelled panels samples with a larger cross section reach 38.3 ± 3.4 MPa ultimate tensile strength and an elongation at failure of 10.2 ± 2.8 %, whereas the densified ones reach 73.7 ± 8.7 MPa and 7.3 ± 1.9 % respectively. Table 1 provides an overview of all the values determined. The values for each of the two kinds of material are averaged because, although different densities of foam cores are calculated, all samples were taken from the same AFS panel. In the samples that have been levelled only, not always both face sheets break at the same time. Rather, after one face sheet fails initially, the other will continue carrying load for continued straining by a few percent. This is the reason for the two-step failure of many samples. This behaviour is rarely observed in the densified samples. For Young's modulus, values of 1.53 ± 0.11 and 3.23 ± 0.59 GPa were obtained for levelled and non-levelled samples, respectively, but due to

reasons discussed later these values are not deemed characteristic for the samples measured and are not included in Table 1.

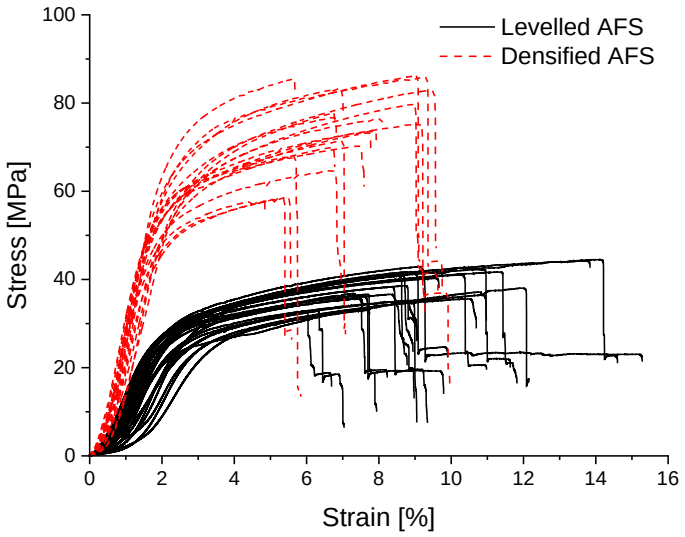

Fig 5 – Stress-strain curves of the tensile tests of foamed and levelled (full black lines) and foamed and densified (dashed red lines) AFS samples.

Table 1 – Summary of the mechanical properties of levelled and densified AFS samples obtained by tensile testing.

Mechanical parameters (tensile)	Levelled AFS	Densified AFS
Number of samples	25	20
Sample thickness (mm)	8.5±0.2	4.5±0.2
Foam core density (g/cm³)	0.49±0.05	1.55±0.13
Yield strength – $R_{p0,2}$ (MPa)	23.7±1.4	50.3±9.0
Ultimate tensile strength – R_m (MPa)	38.3±3.4	73.7±8.7
Strength at rupture – R_B (MPa)	21.4±9.2	51.1±21.5
Strain at rupture – ε_B (%)	10.2±2.8	7.3±1.9

The core of an AFS panel is predominantly a homogeneous foam with a few larger pores as can also be seen in Fig 6a. These pores result in an area of lower density, which becomes visible in the radiography. For a better evaluation of the local density, the false colour image is also presented in Fig 6b. In these samples, the false colour images show that the local density in the upper areas is slightly lower than in the lower ones, visible through an increased presence of yellow patches. Moreover, the rightmost sample shows two pore clusters in the lower half. One could suspect that failure would be more likely in low-density areas. This is the case for the left and right samples in

Fig 6, see c. For almost homogeneous samples such as the one in the middle, no preferential failure site can be identified.

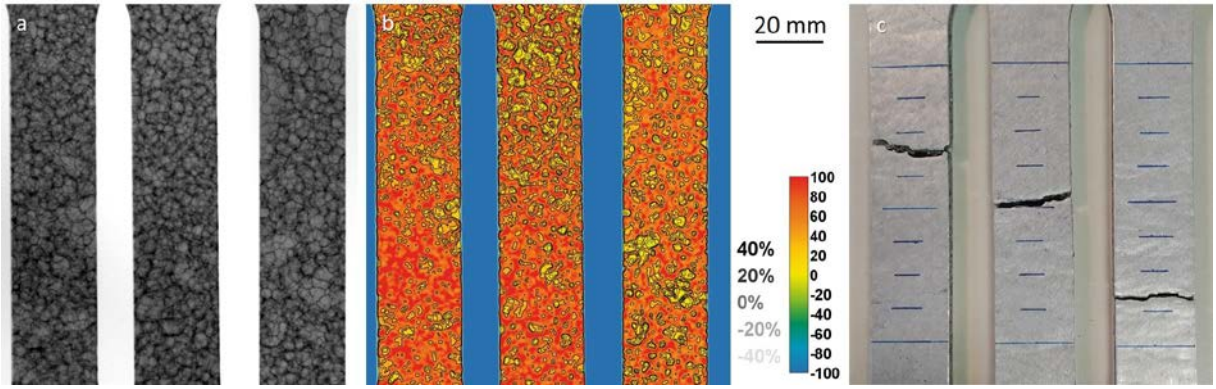

Fig 6 – Three exemplary levelled AFS samples submitted to tensile tests. a) X-ray radiographies of AFS samples before the test, b) false colour image of the X-ray absorption before the test and c) photography of the samples after the tensile tests.

However, some samples contain defects or accumulations of bigger pores, which lead to failure at these positions during the tensile tests. Two such examples are given in Fig 7. Although here densified samples are shown exemplarily, such defects occur in both sample groups. In the left and middle sample in Fig 7a, only slight variations in density are visible other than in the right sample, where an obvious area of low density extends over the entire sample. This area is also clearly visible in the false colour image (Fig 7b). In addition, a lower-density spot can be identified in the middle sample not clearly noticeable in the greyscale image which explains the fracture of the specimen far from the centre. The sample on the right failed as expected. In the sample on the left side, only the top layer on the back broke in the upper third without correlation to any density feature.

In around 50 % of all tensile test samples defects like these could be visually detected in X-ray images and in every second of these cases, failure occurred at such a location. The false colour representation simplifies recognition of local density variations and the correlation with the failure location offers the possibility of an automated recognition once the algorithms have been further improved.

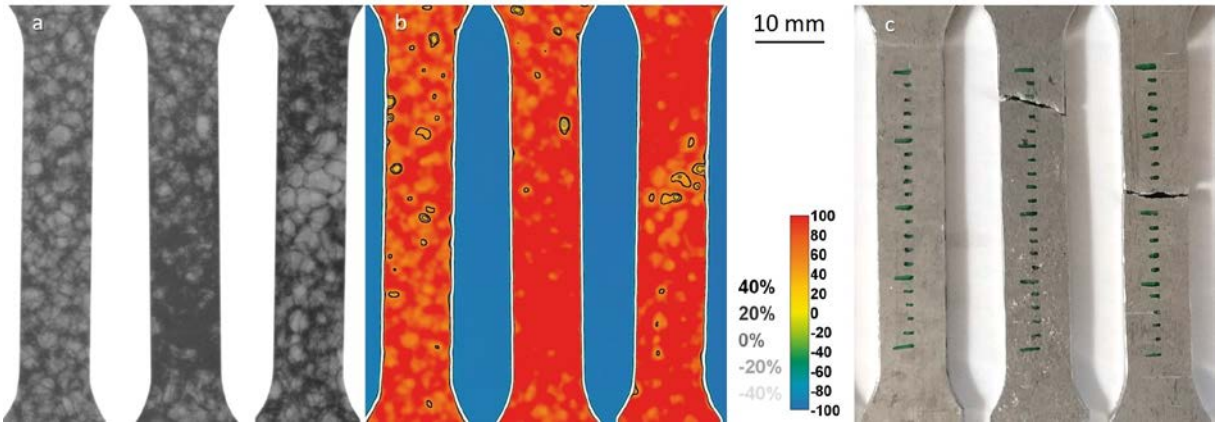

Fig 7 – Three exemplary densified AFS samples submitted to tensile tests. a) X-ray radiographies of samples before the test, b) false colour representations of radiographies before the test, c) photographies of the samples after the tensile tests (sample on left has fractured on back side). Weak density spots in the densified foam structure can be correlated with the failure positions and are marked with circles (green: probability detected beforehand, purple: detection possible in hindsight).

The stress concentration resulting from the absence of mass created through a pore can have a greater influence than classical failure points such as notches or narrowings. Fig 8 shows a sample with a production defect that has such a narrowing in the lower area and a similarly significant spot in the upper area as shown in Fig 7. The measurements on this sample were excluded from the average given in Table 1, but illustrate the problem very well. Failure is in the upper area as can be seen in Fig 8c+d. Although the sample did not fail at the narrowing a crack developed at this site as well as at others.

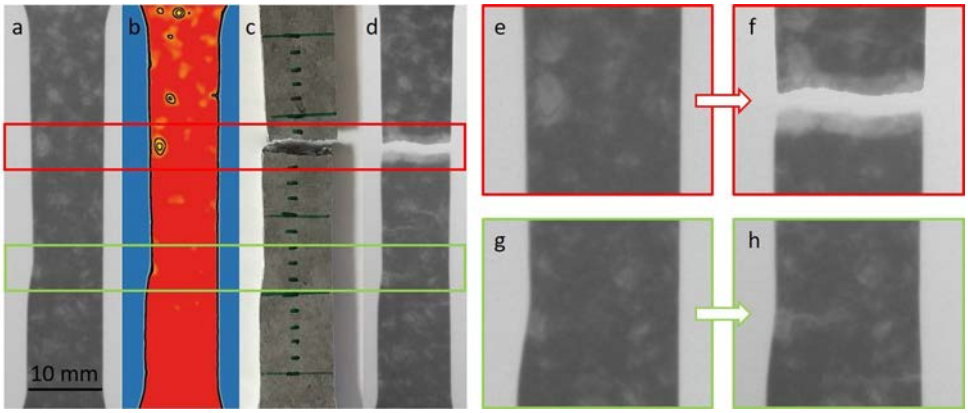

Fig 8 – Densified AFS sample showing a narrowing before the tensile test. a) X-ray radiography, b) false-colour image, c) photo and d) radiography of the same sample after the test. e)-h) magnification of the regions of interest.

These cracks occur over the entire length of the specimen and run perpendicular to the direction of force. This and that they are almost evenly distributed can be observed better in Fig 9. Slight depressions or deformations at these positions can be seen on the face sheets, but no initiation of

cracks themselves. They occur in both the just levelled and the densified samples. In the latter, the cracks are present in larger numbers.

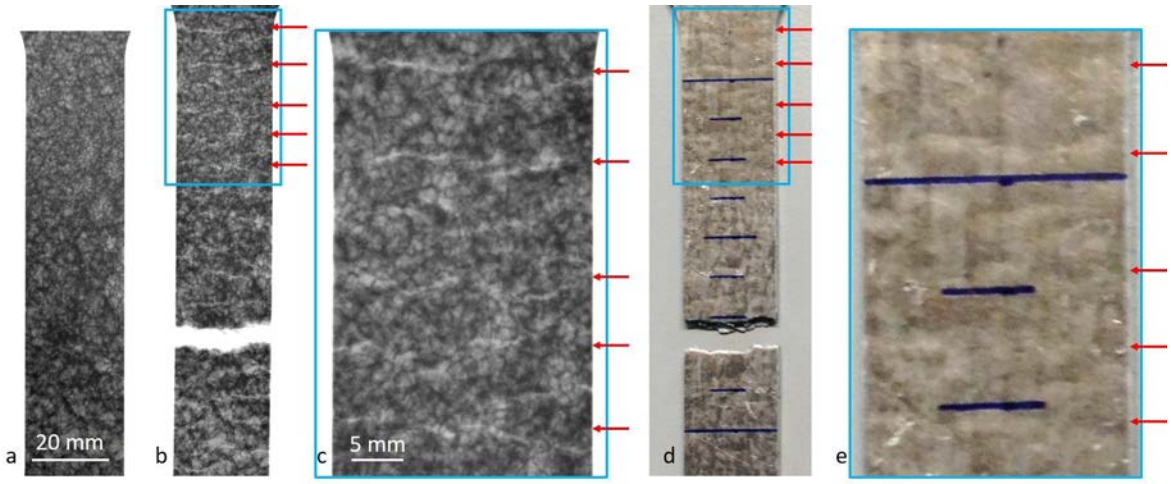

Fig 9 – Internal cracks in a densified AFS sample formed during tensile test. a) X-ray radioscopic image before test, b) radioscopic image after tensile test, c) enlargement of top region of b), d) image of face sheet surface after tensile test, e) enlargement of d).

Compression tests

Compression tests were performed on levelled and non-levelled but not on densified samples. The corresponding stress-strain curves are displayed in Fig 10a. They show the expected behaviour of a cellular material, including that for higher plateau stresses the reachable strain is less. One curve, however, stands out in comparison due to the significantly higher plateau stress. The radiography of this sample is depicted in Fig 10b, 3rd row, 2nd picture. It contains not fully foamed areas, which makes the structure irregular. The density of this sample is higher than that of the others, which can also be recognized by the darker image. Foam densities for all the samples tested range from 0.31 - 0.69 g/cm³. Since all samples came from the same AFS panel, this denser sample is part of the expected fluctuations. All mechanical values determined are given as averages in Table 2.

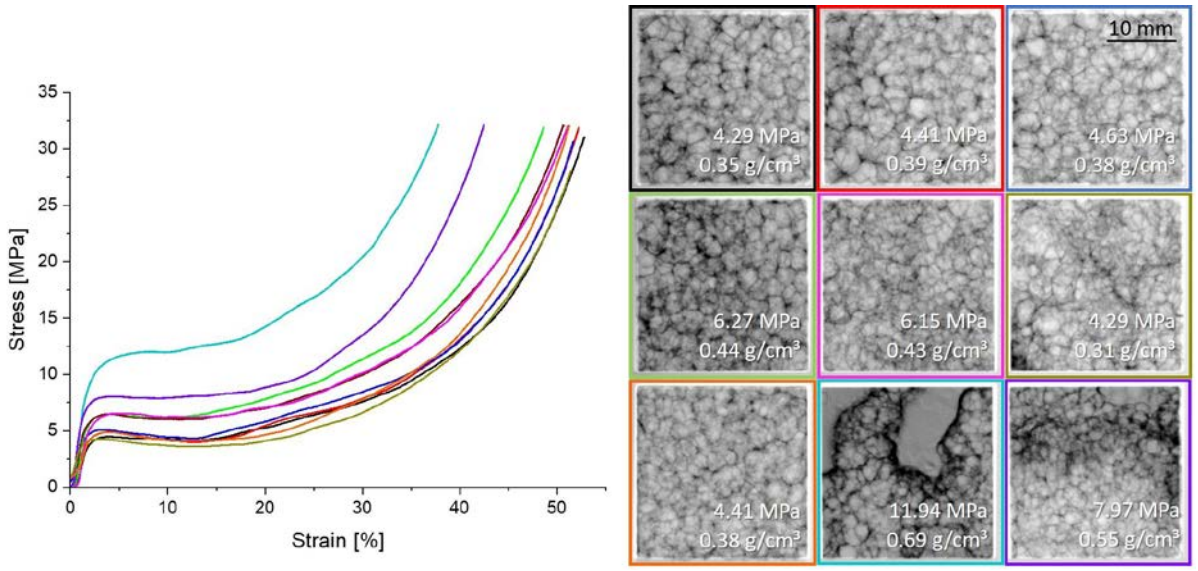

Fig 10 – a) Stress strain curves of compression tests of representative levelled AFS samples (25 mm × 25 mm × 8 mm). b) some X-ray radiographies of samples before the compression test together with the corresponding plateau stress (mean stress between 5 and 13 % strain) and density of foam core.

Since the AFS panels usually have already been subjected to a compressive load by the levelling process, additional tests were carried out with 21 non-levelled samples. The foam core densities of these 21 samples, despite differences in thickness, are calculated to 0.44±0.04 g/cm³. This shows that the large-scale foaming process of the AFS panel production results in an almost homogeneous foam density.

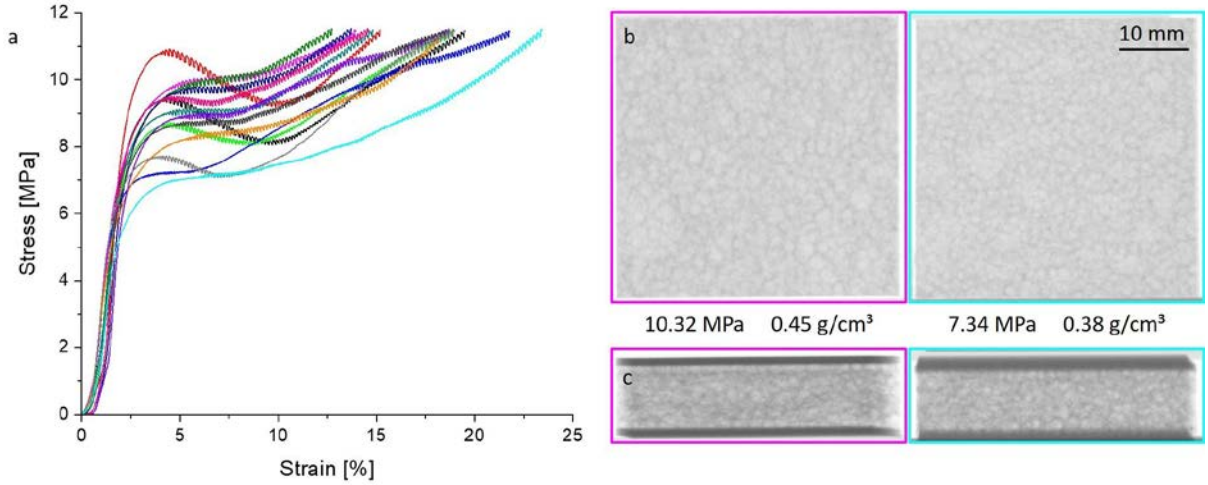

Fig 11 – a) Stress strain curves of compression tests of the non-levelled AFS samples of 40 mm × 40 mm × 12.8 ± 0.9 mm size. b) top and c) side view of X-ray radiographies of both extreme cases with the corresponding maximum and minimum plateau stress.

Due to the larger area of the non-levelled samples, the test load was not sufficient to determine the stress strain curve up to the end of the plateau in every case as can be seen in Fig 11a. In contrast to the levelled AFS samples, a clear drop in the stress strain curve can be observed here for some

samples after the onset of densification. Averages of all the values determined are listed in Table 2. The top and side view of X-ray radiographies of both extreme cases are shown in Fig 11b and Fig 11c. The side view clearly reveals that the first and last layers of pores of the foam are ordered at the boundary with the face sheets, presumably into a packing close to simple cubic and thus the centre of this layer has a lower local density. Young's modulus (structural stiffness) determined from the loading curve is just 620 ± 210 and 660 ± 170 MPa for levelled and unlevelled samples, respectively, which is not considered realistic, see discussion.

Table 2 – Summary of compressive properties of levelled and non-levelled AFS samples obtained from the compression tests. Values determined according to DIN 53291.

Mechanical parameters (compressive)	**Levelled AFS (25 mm × 25 mm)**	**Non levelled AFS (40 mm × 40 mm)**
Number of samples	10	21
Sample thickness (mm)	8.8±0.1	12.8±0.9
Foam core density (g/cm³)	0.43±0.11	0.44±0.04
Yield strength – R_{d1} (MPa)	5.9±1.8	8.9±1.3
Plateau stress – σ_{plt} (MPa)	6.0±2.3	9.1±0.9
Strain at end of plateau region – $\varepsilon_{plt\text{-}E}$ (%)	23.5±1.4	N/A

Four-point bending tests

Failure of samples in 4-point bending tests occurred in almost all specimens between the outer supporting and the inner loading rollers. Only one levelled AFS specimen showed bulging of one face sheet between the two loading rollers. The corresponding stress over deflection curves are shown in Fig 12d. The most prevalent type of failure was shearing of the foam core. This may happen in two ways: across the foam core and/or 'delamination' of one of the two face sheets. The latter term means that no full pore layer adheres to the face sheets after pulling off, but there are always residues of cell walls perpendicular still attached to the sheets. In this sense, the term 'delamination' is a modification of the usual sense that implies a smooth separation of layers. Failure of a combination of both is depicted in Fig 12b. Of the 23 levelled samples, 9 failed by delamination, 5 by core failure and 9 through a combination of both. For the densified samples, it was also possible that instead of core shear one of the face sheets broke (Fig 12c). This happened 12 out of 21 times. Delamination was only observed 3 times. The calculated and averaged mechanical values are given in Table 3.

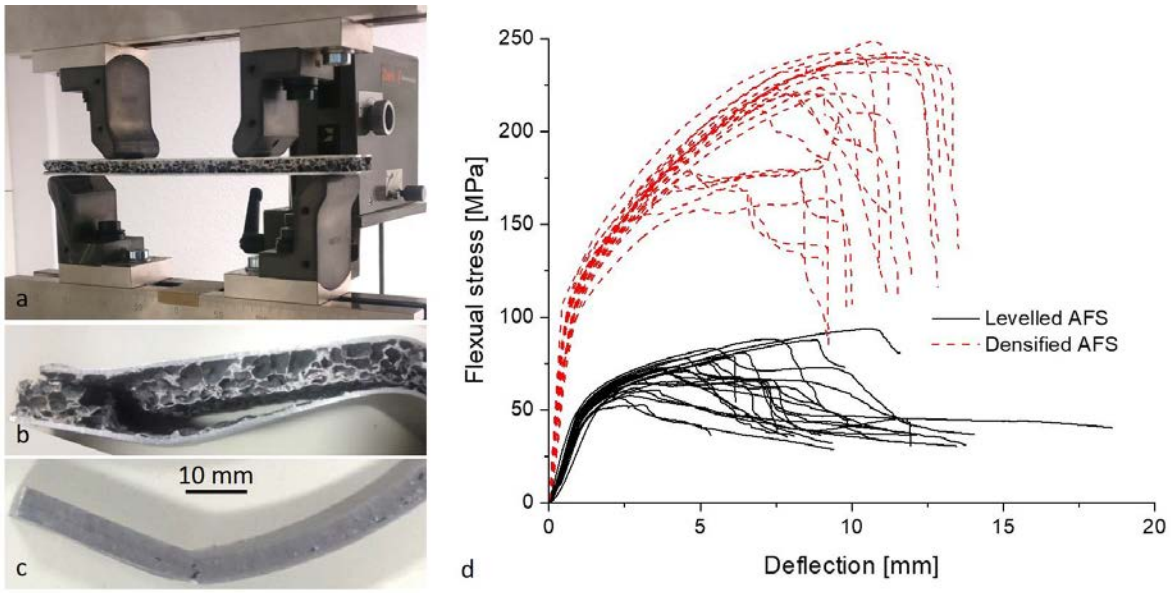

Fig 12 – a) Picture of sample in the bending jars, b) and c) pictures of examples of the corresponding failure regions. d) stress-deflection curve of the 4-point-bending-tests of levelled AFS-samples (full black line) and of densified AFS samples (dashed red line).

In the radiographic images in Fig 13, the structure between the inner loading rollers is depicted. The side view demonstrates that directly next to the surface layer there are denser areas on one side and less dense areas on the other as has been already described above. A correlation between structure and failure was possible in one regard: Of the 18 times in which delamination occurred, 17 times it happened in the denser border area. For the sake of visualisation, the position and propagation distance of the delamination occurring in the test have been marked with an orange line in the radiograph taken before testing in Fig 13.

Table 3 – Summary of the mechanical properties of levelled and densified AFS samples obtained from four-point-bending-tests. Values determined according to DIN 53293.

Mechanical parameters (4-point bending)	**Levelled AFS**	**Densified AFS**
Number of samples	23	21
Sample thickness (mm)	8.4±0.1	4.7±0.2
Foam core density (g/cm³)	0.46±0.06	1.42±0.16
Flexural modulus – E_f (GPa)	21.7±1.9	33.6±3.8
Flexural yield strength – $\sigma_{0,2}$ (MPa)	62.6±4.2	108.9±6.2
Max. flexural stress – $\sigma_{f,max}$ (MPa)	72.0±10.7	206.8±60.1
Flexural stress at failure – $\sigma_{f,B}$ (MPa)	38.1±7.0	133.7±41.1
Strain at failure – ε_B (%)	2.4±0.6	5.2±0.8

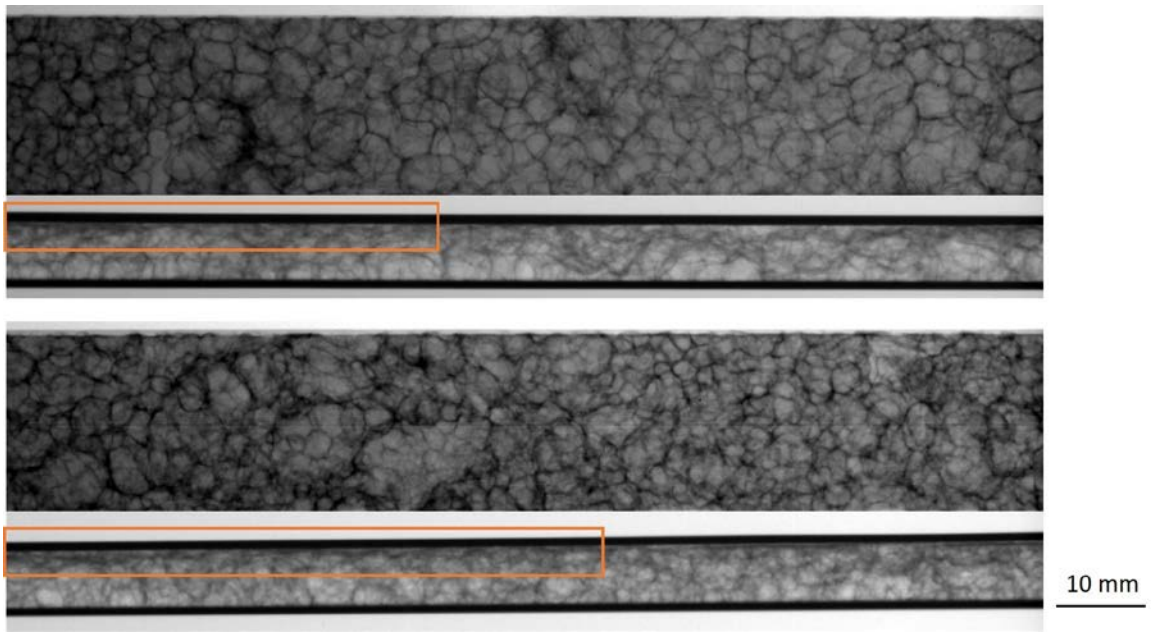

Fig 13 – X-ray radiographies of two exemplary AFS samples before the four-point-bending test, top and side view. Orange line shows where delamination will happen.

Discussion

Levelling

Levelling equalises differences in thickness. Depending on which level thickness differences must be compensated, a considerable amount of material movement might be necessary. Since levelling is carried out at elevated temperatures, the cell walls do not necessarily break but can deform at least partially plastically. As shown in Fig 2c, bands of deformed or compressed pores can form. This has already been reported in the literature [13][14], where bands have been associated with locally weaker pores. For thinner AFS panels as shown in Fig 3 compressed bands usually form near a face sheet. This can be explained by the nature of the levelling process: In thin AFS panels, the smaller thickness results in a lower number of pores and in particular the last pore layer is aligned to the face sheets due to geometrical restrictions [17]. Due to their lower local density (bubbles are ordered at the face sheet and have a more open packing unlike in the interior of a foam where packing densities approach the densest possible packing) such layers are easier to deform than the regions in the interior of an AFS plate. In fact, both layers can be deformed as shown in Fig 3 by the pores marked in red. Frequently, one of these two layers is more noticeably deformed, see Fig 13. This can be explained by the specific conditions of levelling: After foaming they first cool during transfer to the levelling press, into which they are put onto a horizontal plate and re-heated up to the desired temperature before pressing them to their end thickness. In order to avoid a large temperature gradient and premature deformation of the upper side of the panel during heating, the upper plate

of the press is usually positioned slightly above the upper face sheet. With this procedure, the lower face sheet is hotter and therefore the first neighbouring pore layer is slightly weaker than the upper one due to a better thermal contact to the bottom press plate and therefore mostly yields first.

In AFS panels with thicker foam cores, a pore layer more towards the centre of the panel is more likely to yield first. The reason is probably that the heat from the foaming process remains in those regions for a longer time, which are therefore weaker and more prone to be deformed during levelling. This is favourable for higher bending stiffness as in this way delamination close to the face sheet can be avoided.

In future the need for levelling may become obsolete if the foaming and levelling was to be done in one step. A precise temperature control inside the precursor and distance control of the levelling press would be necessary and even then a homogenous pore structure would not be guaranteed.

Panel densification

In the levelled and densified samples, the entire foam core is deformed by pressing into a denser plate. The density of the core reaches 1.55 ± 0.21 g/cm³ on average. The remaining porosity is close to 40 % or lower. In the cross section of the cut sample in Fig 2c on the right, only a few cell walls are recognizable, which are mostly parallel to the face sheets. This is also a reason for the slightly blurred X-ray images of the densified samples (compare Fig 2d), as there are almost no more cell walls perpendicular to image plane left any more, which could deliver a sharp contrast.

Tensile tests parallel to face sheets

The measured yield and ultimate tensile strength values are low compared with bulk aluminium. However, if we assume that the face sheets bear the load exclusively and extrapolate the theoretical properties of the face sheet alloy at T451 [18] to the extended cross-section of the AFS sample according to the Voigt model, we obtain values that lie slightly above the measured values of the levelled AFS samples, see Table 4. This applies similarly to the densified AFS samples.

Table 4 – Comparison of the mechanical properties of levelled AFS samples with theoretical values.

Mechanical parameters (tensile)	**Levelled AFS**	**Theoretical values of EN AW 6082 T451** [18]**, extrapolated to AFS cross section**
Young's modulus (GPa)	1.53±0.11	12,9
Yield strength – $R_{p0,2}$ (MPa)	23.7±1.4	28,1
Ultimate tensile strength – R_m (MPa)	38.3±3.4	45

This soft state is a consequence of the heating cycles required for foaming and levelling. However, it was shown that it is possible to heat treat the face sheets of AFS again [19] so that this restriction can

be overcome. As the strength of the face sheets is not known, the contribution of the foam core cannot be calculated. The discrepancy between the Young's moduli of almost one order of magnitude can be due to a minute yielding of the foam core to the clamping forces of the testing fixtures and the corresponding movement in the testing direction. It was minimized by infiltrating the foam core with epoxy resin in the clamping region but could not be completely excluded. Another difference is clearly visible in the elongation at break. This should be at least 19 % for the above-mentioned strength class. Since the gauge lengths were identical for both sample types, compression or levelling seems to damage the foam core, which will lead to earlier fracture. As shown in Fig 9, the foam core has developed cracks all over the length of the sample before failure. Single cell walls and Plateau borders already broken during foam solidification [20][21] may act as seeds for crack propagation. The core material fails earlier than the face sheets as seen by the multiple non-fatal crack development in Fig 9, which supports the above assumption that the face sheets bear most of the load. The core and the face sheets are metallically bonded. If the crack tip extends only minimally into the face sheet, this can lead to a stress concentration and an earlier failure. Since these cracks occur more frequently in the densified samples, the probability of failure is higher there, which leads to a lower elongation at break.

Correlation of tensile tests with X-rays

In half the cases in which defects were identified in the foam core, X-ray inspection does not allow to predict where a part will fail. Predictions are even more difficult if samples are very uniform concerning their pore structure. On the other hand, the thickness of the face sheets cannot be determined well with a mere top view, as well as the defects therein cannot be identified. Since the face sheets carry the main part of the load, their properties are crucial for tensional and bending performance of the samples. Small material defects, which are insignificant in the starting material, can become significant by rolling down. It is also possible that a large cavity extending over the entire width of the sample does not lead to failure at its location because the face sheets are a little thicker at this point. As shown in Fig 7 and Fig 8 for certain defects or pore accumulations, the assumption that a part will break there can be made. In 45 % of the cases, the prediction made by the author was correct. Fig 8 also shows that narrowing may be not as significant as the pore structure.

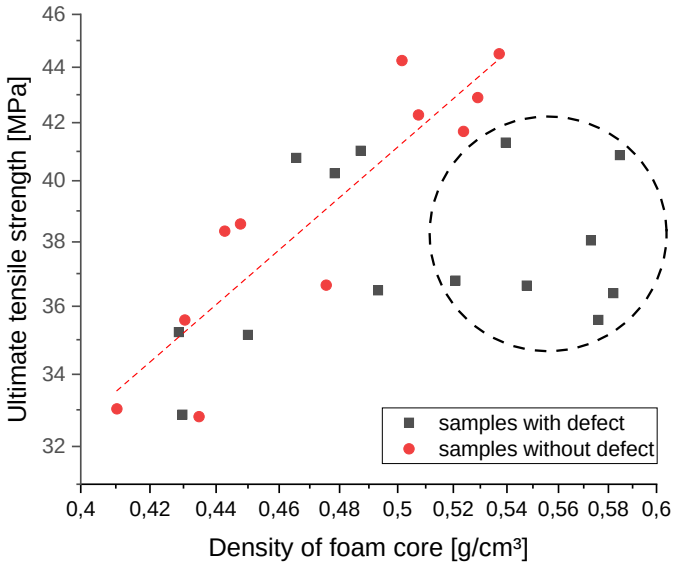

Fig 14 – Ultimate tensile strength along the face sheets of levelled AFS samples. Samples marked in red are those in which the X-ray radiographic visualisations did not show obvious defects, the remaining samples are given in black. The fitted dashed red line connects all samples except the encircled ones, see discussion in text, and represents approximately a linear function of density.

The ultimate tensile strength of levelled AFS samples, see Fig 14, exhibits a trend of higher strength for higher foam core densities. This dependency is not as pronounced as for compression tests since a large part of strength originates in the face sheets. If one distinguishes between samples in which X-ray radiography showed no defects from those with defects we notice that the latter group includes samples with a weaker performance (encircled points) than that of the former where the density dependence approximately follows the red broken line. In other words, samples showing defects in the radiographic images are more likely to underperform in tensile tests, however, not all do so, just roughly 50% of the samples containing defects visible in X-ray images.

By eliminating material that shows defects after radiographic analysis integrated into industrial AFS production, one could reduce the risk of using weak material to build components based on AFS. Discarding material does not necessarily imply that entire AFS panels have to be abandoned since by applying smart cutting strategies a large part of the AFS could still be used even if there are local defects.

Compression tests perpendicular to face sheets

The compression tests suggest that a homogeneous foam structure is not the most important requirement for a good compression resistance. This means that also larger areas of non-homogenous foams structure do not inhibit the use in mainly compressively loaded applications if the core density is not reduced. Unlike in tests parallel to the face sheets, only the foam core and not the face sheets determines the compressive strength of the AFS samples as the foam is the weakest

link. Fig 10 indicates that the compression strength values depend strongly on the foam density as reported before many times, e.g. Refs. [3][22]. This dependence is also depicted in Fig 15, where the plateau stress is plotted against foam density of each levelled and non-levelled AFS sample.

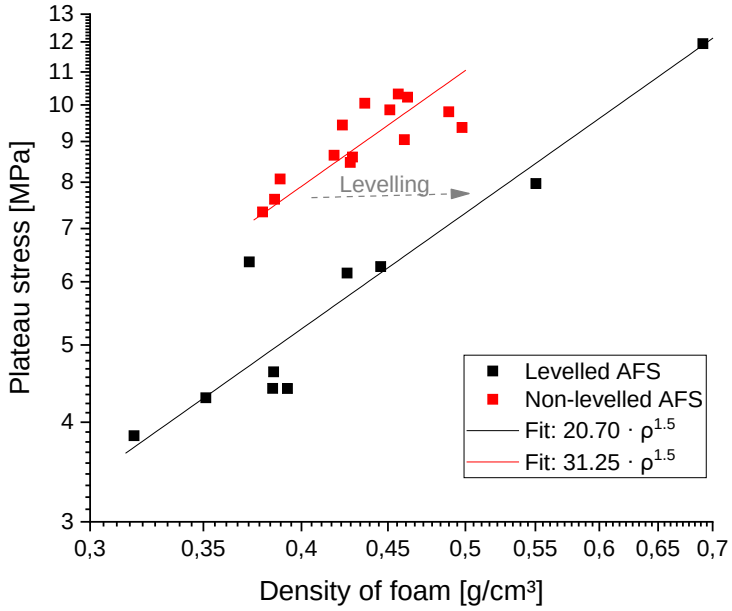

Fig 15 –Plateau stress of compression tests plotted against foam density of AFS sample for levelled (black points) and non-levelled (red points) samples.

Fitting a power law into Fig 15 for the levelled AFS samples yields a function to the power of 1.5. Due to the small density range of the non-levelled samples a fit of the exponent was not reasonable so that just the pre-factor was fitted. This is in good agreement with the Gibson-Ashby model, which gives the plateau stress as a function of density to the power of 1.5 for open porosity foams [3]. The linear term for closed porosity was neglected as the percentage of mass in the cell walls is not known (and probably small). Such pre-factors of 31.25 and 20.70 for the non-levelled and levelled samples respectively are close to the pre-factor for a foam made of AlSi6Cu6 of 24.57 determined by Lehmhus et al. [23], who used the same formula for fitting. The prior deformation associated with levelling increases the density of the foam core while the plateau stress is increased only slightly.

The measured compressive strength of the foam is in the range of other aluminium foams of this density range as given in the literature [22][23][24][25][26]. The compressive stiffness measured without hysteresis is not ideal and low compared to data obtained by other methods of measurement but the values are similar to measurements done in a likewise manner [27]. Young's moduli derived from simple loading curves include large non-reversible contributions in early loading stages that can be avoided by measuring the frequencies of flexural vibrations or sound velocities [28]. A corresponding analysis of AFS samples without face sheets resulted in a Young's modulus of 3.3 GPa for the foam core [29] instead of the 660 MPa as quoted above.

Densification strains given in the literature usually range from 40 % to 70 %. But the measurements there do not include face sheets whose deformation is negligible. Calculating the strain for the foam thickness only results in a strain at the end of the plateau of 30.4 ± 1.8 %. This is still lower than in the literature, but these samples where already compressed during levelling (non-levelled samples did not reach the end of densification).

Four-point bending tests

The four-point bending tests have shown the effects of levelling on the performance of the samples. All levelled samples failed in the foam core. A direct correlation of the failure mode with the pore structure was not possible as has been already reported [30]. If a foam yields in the band of deformed pores a crack spreads only in the band. Almost no deformation is observed in the remaining foam core. This was defined as delamination because the foam is metallically bonded to the face sheets, which inhibits delamination at the interface. If failure originates elsewhere in the foam core, the crack extends until it reaches the band of crushed pores and propagated into it. This is true for all but one sample. This suggests that in this band some cell walls are already weakened or even broken before the bending test, which facilitates the propagation of the crack. The four-point-bending-tests in this paper show similar curves as reported by d'Urso et al. [30].

The densified samples failed in two ways. On the one hand, the samples sheared in the core, spreading the crack into the compressed cells, but not as pronunced as in the levelled AFS samples. This happened only in the sample with a core density less than 1.54 g/cm³. On the other hand, the face sheet sometimes also broke, see Fig 12c. The latter was the sole reason of failure in samples with a core density above 1.61 g/cm³. In the three occasions delamination was observed, the core density was less than 1.3 g/cm³. Compaction of the samples is therefore not the reason for the long propagation distance of the crack. Folding of cell walls over and into each other even partly prevents propagation. Partial compression, the resulting flattening of the pores and possible breakage of the cell walls promotes crack propagation by removing obstacles. The failure modes correspond quite well with the map given by Chen et al. [31].

Homogeneity and quality control

Proper foaming of AFS precursors depends on many factors including that the foam does not expand completely uniformly. This might be caused by: i) The blowing agent may not be distributed evenly during mixing. ii) The density of the precursor may differ slightly due to variations in the powder compaction or rolling step. iii) Slight differences in the face sheet thickness might result in varying precursor thicknesses. iv) slight temperature differences over the area of the AFS during foaming in the furnace. It is therefore not surprising that a foaming process results in areas of different

thicknesses, especially in large commercial panels as shown in Fig 4. Such inhomogeneities are still not completely preventable today and, therefore, a continuous quality control is recommendable, especially when the application envisaged involves safety relevant parts. With non-destructive X-ray examination, faulty or mechanically weak areas can be detected and parts excluded from further use. The detection of defects could also be partially automated. This could minimize material waste and thus also reduce costs. Further improvement of the detection procedures, however, are necessary.

Conclusions

Large aluminium foam sandwich panels (AFS) were foamed, levelled and in some cases partially densified. The foam structure was analysed with X-ray radiography and tomography and correlated to the mechanical behaviour for a large number of samples. We find:

- Depending on the thickness of the AFS panels, the location of the pores flattened during compression or levelling changes: For thin panels almost directly next to the face sheets, for thicker panels mostly in the interior of the foam core. Samples partially densified can bear higher stresses but the possible strain levels are reduced. They are the best choice for joining points.
- X-ray radioscopy allows us to screen samples for defects that might become weak links in the AFS panel in use. In 50% of all samples, no such defects are discovered and the foams appear uniform. In the other cases defects occur. Of these about 50 % give rise to a predictable localised failure, in the other cases not.
- Roughly half of the samples in which a defect occurs underperform in tensile tests. The others perform as samples without defects detected in X-ray radioscopy. None of the latter samples underperformed.
- Tensile behaviour parallel to the face sheets exhibits notable deformation potential unlike bare foams.
- Compressive strength is not primarily given by the uniformity of foam structure but by foam density. The stress-density dependence of AFS corresponds to what is known from the literature for bare foams without face sheets [3].
- During 4 point-bending delamination occurs mostly in the denser, slightly compacted layers of the levelled samples.
- X-ray screening should be included in industrial AFS production since it can lower the risk of using underperforming flawed samples

Data Availability

The experimental data are available from T.R.N. or F.G-M. upon reasonable request.

Conflicts of Interest

The authors declare no conflict of interest.

References

[1] J. Banhart and H.-W. Seeliger, “Aluminium foam sandwich panels: Manufacture, metallurgy and applications,” *Adv. Eng. Mater.*, vol. 10, no. 9, pp. 793–802, 2008.

[2] M. F. Ashby, A. G. Evans, N. A. Fleck, L. J. Gibson, J. W. Hutchinson, and H. N. G. Wadley, *Metal Foams: A Design Guide*. Butterworth-Heinemann, 2000.

[3] L. J. Gibson and M. F. Ashby, *Cellular Solids: Structure and Properties*, 2nd Editio. Cambridge University Press, 1999.

[4] J. Banhart, “Manufacture, characterisation and application of cellular metals and metal foams,” *Prog. Mater. Sci.*, vol. 46, pp. 559–632, 2001.

[5] J. Banhart, F. García-Moreno, K. Heim, and H.-W. Seeliger, “Light-Weighting in Transportation and Defence Using Aluminium Foam Sandwich Structures,” in *Light Weighting for Defense, Aerospace, and Transportation*, A. A. Gokhale, N. Eswara Prasad, and B. Basu, Eds. Springer Nature, 2019, pp. 61–72.

[6] F. García-Moreno, “Commercial Applications of Metal Foams: Their Properties and Production,” *Materials (Basel).*, vol. 9, no. 2, p. 27, 2016.

[7] J. Banhart and H.-W. Seeliger, “Recent trends in aluminum foam sandwich technology,” *Adv. Eng. Mater.*, vol. 14, no. 12, pp. 1082–1087, 2012.

[8] X. H. Han, Q. Wang, Y. G. Park, C. T’Joen, A. Sommers, and A. Jacobi, “A review of metal foam and metal matrix composites for heat exchangers and heat sinks,” *Heat Transf. Eng.*, vol. 33, no. 12, pp. 991–1009, 2012.

[9] H.-P. Degischer and B. Kriszt, Eds., *Handbook of Cellular Metals - Production, Processing, Applications*. Wiley-VCH, 2002.

[10] H.-W. Seeliger, “Method for producing a semi-finished product for a composite material,” WO 2019053192A1, 2019.

[11] D. Schwingel, H.-W. Seeliger, C. Vecchionacci, D. Alwes, and J. Dittrich, “Aluminium foam

sandwich structures for space applications," *Acta Astronaut.*, vol. 61, pp. 326–330, 2007.

[12] F. Garcia-Moreno, M. Fromme, and J. Banhart, "Real-time X-ray Radioscopy on Metallic Foams Using a Compact Micro-Focus Source," *Adv. Eng. Mater.*, vol. 6, no. 6, pp. 416–420, 2004.

[13] M. Kolluri, S. Karthikeyan, and U. Ramamurty, "Effect of lateral constraint on the mechanical properties of a closed-cell al foam: I. Experiments," *Metall. Mater. Trans. A Phys. Metall. Mater. Sci.*, vol. 38 A, no. 9, pp. 2006–2013, 2007.

[14] M. Mukherjee, M. Kolluri, F. Garcia-Moreno, J. Banhart, and U. Ramamurty, "Strain hardening during constrained deformation of metal foams - Effect of shear displacement," *Scr. Mater.*, vol. 61, no. 7, pp. 752–755, 2009.

[15] P. H. Kamm, "Der Schäumprozess von Aluminiumlegierungen : Tomoskopische Untersuchung der Gasnukleation," Dissertation - Technische Universität Berlin, 2018.

[16] I. T. Jolliffe, *Principal components analysis*, 2nd Editio. Springer-Verlag, 2002.

[17] F. Garcia-Moreno, M. Mukherjee, C. Jiménez, A. Rack, and J. Banhart, "Metal Foaming Investigated by X-ray Radioscopy," *Metals (Basel).*, vol. 2, pp. 10–21, 2012.

[18] W. F. Gale and T. C. Totemeier, Eds., *Smithells Metals Reference Book*, 8. Auflage. Elsevier Butterworth-Heinemann, 2004.

[19] S. G. Shabestari, N. Wanderka, H.-W. Seeliger, and J. Banhart, "Optimisation of the Strength of Aluminium Foam Sandwich (AFS) Panels by Different Heat Treatments," *Mater. Sci. Forum*, vol. 519–521, pp. 1221–1226, 2006.

[20] M. Mukherjee, F. Garcia-Moreno, and J. Banhart, "Defect generation during solidification of aluminium foams," *Scr. Mater.*, vol. 63, pp. 235–238, 2010.

[21] J. Lázaro, E. Solórzano, M. A. Rodríguez-Pérez, and F. García-Moreno, "Pore connectivity of aluminium foams : effect of production parameters," *J. Mater. Sci.*, vol. 50, no. 8, pp. 3149–3163, 2015.

[22] N. Wang *et al.*, "Compressive performance and deformation mechanism of the dynamic gas injection aluminum foams," *Mater. Charact.*, vol. 147, pp. 11–20, 2019.

[23] D. Lehmhus, M. Busse, Y. Chen, H. Bomos, and H. W. Zoch, "Influence of core and face sheet materials on quasi-static mechanical properties and failure in aluminium foam sandwich," *Adv. Eng. Mater.*, vol. 10, no. 9, pp. 863–867, 2008.

[24] E. Andrews, W. Sanders, and L. J. Gibson, "Compressive and tensile behaviour of aluminum foams," *Mater. Sci. Eng. A*, pp. 113–124, 1999.

[25] H. P. Degischer, U. Galovsky, R. Gradinger, R. Kretz, and F. Simancik, “Ueber die Eigenschaften von Aluminiumschaeumen,” in *Conf. Proceedings: Metal foams*, 1997, pp. 79–90.

[26] D. Lehmhus, M. Vesenjak, S. de Schampheleire, and T. Fiedler, “From stochastic foam to designed structure: Balancing cost and performance of cellular metals,” *Materials (Basel).*, vol. 10, no. 8, p. 922, 2017.

[27] I. Duarte, M. Vesenjak, L. Krstulović-Opara, and Z. Ren, “Static and dynamic axial crush performance of in-situ foam-filled tubes,” *Compos. Struct.*, vol. 124, pp. 128–139, 2015.

[28] Bernd Weiler and C. U. Grosse, “Elastic constants - their dynamic measurement and calculation,” *Otto-Graf-Journal*, vol. 6, pp. 116–131, 1995.

[29] C. Liebold, “Größeneffekt in der Elastizität – Experimentelle , analytische und numerische Untersuchungen,” Dissertation - Technische Universität Berlin (in German), 2015.

[30] G. D’Urso and G. Maccarini, “The formability of aluminum foam sandwich panels,” *Int. J. Mater. Form.*, vol. 5, no. 3, pp. 243–257, 2012.

[31] C. Chen, A. M. Harte, and N. A. Fleck, “Plastic collapse of sandwich beams with a metallic foam core,” *Int. J. Mech. Sci.*, vol. 43, no. 6, pp. 1483–1506, 2001.